Journal of Materials Chemistry C

PAPER

View Article Online
View Journal | View Issue

Cite this: J. Mater. Chem. C, 2014, 2, 6618

Interacting networks of purely organic spin–1/2 dimers†

Yulia B. Borozdina,‡[a] Evgeny Mostovich,[ab] Volker Enkelmann,[a] Bernd Wolf,[c] Pham T. Cong,[c] Ulrich Tutsch,[c] Michael Lang[c] and Martin Baumgarten*[a]

Received 27th February 2014
Accepted 25th June 2014

DOI: 10.1039/c4tc00399c

www.rsc.org/MaterialsC

In the present study we report the synthesis of some novel nitronyl nitroxide biradical systems **1–4c** with various π-bridges between the radical centres. UV-Vis, IR, EPR and X-ray diffraction studies, along with MS and NMR data where appropriate, are described. Magnetic measurements revealed that the biradicals **1c**, **3c** and **4c** exhibit a moderately strong antiferromagnetic *intra*-molecular exchange, whereas nitroxide **2c** shows a significantly higher exchange coupling, which can only be explained by the presence of strong *inter*-molecular interactions. From DFT calculations performed on the basis of the X-ray crystal structure of compound **4c**, a theoretical value of the *intra*-dimer coupling constant $J_{intra} = -8.6$ K is obtained. Direct proof also for *inter*-molecular arrangement with $J_{inter} \sim -2$ K was provided by the low temperature AC studies of biradical **4c**. According to the magnetic characterization, the nitronyl biradical **4c** is a promising candidate for a purely organic-based low-dimensional quantum magnet.

Introduction

Recently, coupled spin–dimer systems composed of closely-spaced pairs of spin-1/2 carrying entities, have been used as model systems for exploring critical phenomena under well-controlled conditions.[1] As a prominent example of special features observed here we mention the field-induced delocalization of bosonic excitations in reduced dimensions. Likewise, for three-dimensional spin–dimer networks, these systems can be used to study the phenomenon of Bose-Einstein condensation (BEC) of magnetic excitations.[1]

The most commonly used spin carriers for constructing magnetic materials are metal ions and nitroxide radicals.[2] Hence, various approaches toward molecular magnets can be classified into inorganic and organic ones, where the spins are provided by metal ions, the so-called "metal-radical" or hybrid approach, which combines magnetically active metal ions and persistent organic radicals as ligands,[3,4] and the organic approach,[5] with purely organic radical entities. Inorganic materials have some drawbacks, as the size of the cluster, which can be compressed only till a certain limit, and that the structure of the complex is difficult to predict depending on serendipity. On the other hand, organic compounds are usually transparent in many regions and could be obtained in optical active chiral forms.[4] Thus, they might be used as magneto-optical switches and for the manipulation of polarized light in optical devices. Latterly they were extensively studied due to their potential application as radical-based batteries,[6–8] electric conductors[6,9,10] and spintronic devices.[6,9,11]

Importantly, chemistry techniques permits to perform structural modifications in organic materials in order to control the *intra*- and *inter*-molecular exchange interactions between the spin carriers.[5] Thus, the former can be designed and adjusted through synthesis of different conjugated bridges between the spin-containing sites, although the latter requires supramolecular approaches employing hydrogen bonding, π-stacking, and metal complexation. Such tunability is unprecedented in most of the traditional inorganic materials and is the key to obtain materials with unique magnetic properties.

As the spin carrier we have chosen nitronyl nitroxide (NN) radicals,[1] due to their thermal and environmental stability and chelating properties. As in other biradical species, such as imino nitroxide, verdazyl or *tert*-butyl nitroxide radicals, the spin density of the unpaired electron is delocalized over two sites of coordination, leaving open the possibility to arrange molecular units into a supramolecular network with unprecedented magnetic structure.[12,13]

In our study we considered organic spin–dimer systems with singlet ground state and moderate *intra*-dimer interactions in

[a]Max Planck Institute for Polymer Research, Ackermannweg 10, 55128 Mainz, Germany
[b]Novosibirsk Institute of Organic Chemistry Siberian Branch of the Russian Academy of Science, Lavrentiev avenue 9, 630090 Novosibirsk, Russia
[c]Physikalisches Institut, Johann Wolfgang Goethe- University Frankfurt, 60438 Frankfurt am Main, Germany

† Electronic supplementary information (ESI) available: Fig. S1–12 UV-Vis spectra of the nitronyl nitroxides **1–4c**, IR spectra of dialdehyde **4a**, imidazolidine **4b**, biradicals **2c**, **3c** and **4c**, EPR spectra of the biradical **3c**, magnetic susceptibility data of compounds **1–3c**, TOC graphic of **4c**, respectively. CCDC 822066, 816633, 816635. For ESI and crystallographic data in CIF or other electronic format see DOI: 10.1039/c4tc00399c

‡ Present address: Institute of Biochemistry, Ernst-Moritz-Arndt University Greifswald, Felix-Hausdorff-Straße 4, 17487 Greifswald, Germany.

the range of −2 to −8 K (the numbers refer to the exchange coupling defined in accordance with the Hamiltonian used in the DFT calculations). In addition, the compounds should form interacting networks due to small *inter*-dimer interactions, giving rise to field-induced magnetic states, depending on the dimensionality of the interactions, at fields below the saturation field.[2] Since it is difficult to predict the precise magnitude of the *intra*- and *inter*-molecular exchange interactions, which can further affect the strength of the bulk magnetic coupling, we started from approximate computational estimations based on the coordination geometry and the bond distances in the molecules, and have targeted four biradicals for in-depth characterization.

Herein we report the synthesis of biradicals **1c–4c**, designed for the fine tuning of spin exchange interactions, their characterization, including X-ray structural analysis, and, finally, the magnetic studies, which are discussed with respect to the quantum chemical calculations based on a broken symmetry DFT approach.

Results and discussion

Synthesis of biradicals

The synthesis of the nitronyl nitroxide radicals (NN) relies, in general, on the condensation between 2,3-bis(hydroxyamino)-2,3-dimethylbutane (BHA) with an aldehyde functional group, followed by the oxidation reaction of the condensation products (Fig. 1). In order to achieve fine tuning of the magnetic exchange interactions in biradical systems, we used conjugation control of the bridging unit with topologically aligned radicals in the *para*-position. Theoretical studies emphasized the importance of the mutual orientation and relative distances in the crystal packing for the unimpeded magnetic coupling propagation.[13] We engineered four novel π-conjugated formyl derivatives (**1a–4a**), the key precursors towards NN synthesis, *via* diverse multi-steps approaches, as outlined in Schemes 1–4. These π-conjugated systems vary from each other, and can be divided into three different classes. The first group (i) contains electron-donor substituents, which are able to increase the electron density along the spin-coupling backbone (radical **1a–c**,

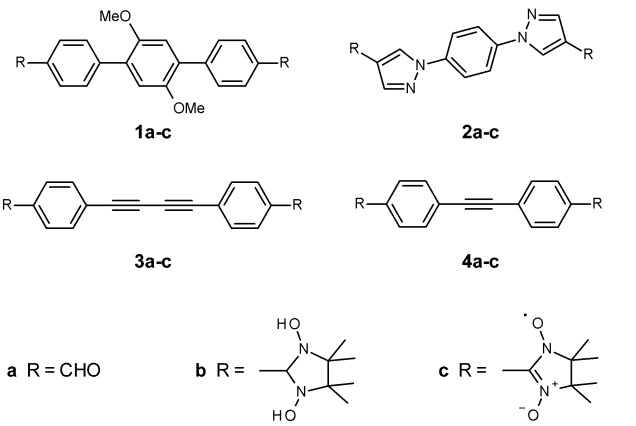

Fig. 1 Model compounds **1–4** with emphasized bridging units.

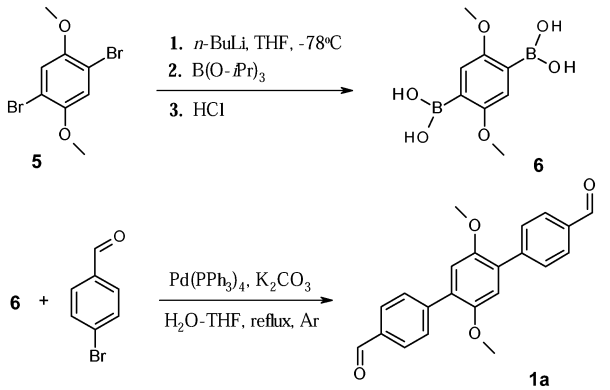

Scheme 1 Synthetic route towards dialdehyde **1a**.

dimethoxyphenyl-derivatives). Class (ii) is made by rigid and planar molecules (compounds **3** and **4**, in other words, acetylene derivatives). Finally, group (iii), which includes five-membered hetero-rings as functional part of the coupling unit, which provides non-alternate spin-polarization paths (compound **2a–c**, pyrazole derivatives).

Synthesis of the first target dialdehyde **1a** (class (i)) is represented in Scheme 1. Regardless of the different coupling conditions tested, the 4-[4-(4-formylmethyl)-2,5-dimethoxyphenyl]benzaldehyde (compound **1a**) could not be synthesised *via* direct coupling of the dibromo derivative **5** with 4-formylbenzeneboronic acid. In fact, only the mono-substituted product was isolated at best. Thus, an alternative route was explored successfully, as shown in Scheme 1. Initially the dimethoxyether **5** was treated with *n*-BuLi in dry THF at low temperature ($T = -78$ °C), and reaction mixture was left stirring under argon atmosphere at the same temperature for 5 hours. At the end of this time period excess of boron triisopropoxide (tri(propan-2-yloxy)borane) was added dropwise. The mixture was treated with 5% HCl, which afforded diboronic acid derivative (compound **6**) as white solid. Here, the resonance ^{1}H-NMR signal of the hydroxy groups (OH) present in the isolated product falls at 7.82 ppm and confirmed, therefore, formation of the desired derivative. The compound was furthermore recrystallized from H_2O–CH_3CN (1 : 1) mixture, affording highly pure derivative **6** in a fairly good yield (45%).

Diboronic acid **6** was then used in the Suzuki coupling reaction with 4-bromobenzaldehyde. The dialdehyde **1a** was obtained only after prolonged reaction under reflux (5 days) in 62% yield. The ^{1}H-NMR spectrum of **1a** shows the appearance of new signals in the aromatic region, at 7.80 and 7.95 ppm, together with ^{1}H-resonance signal at 10 ppm, which is the clear fingerprint for the presence of undamaged aldehyde moieties.

Scheme 2 outlines the synthetic route towards 4-formyl-1-[4-(4-formyl-1*H*-pyrazol-1-yl)phenyl]-1*H*-pyrazole (compound **2a**, class (iii)). The reaction of 1,4-dibrombenzene **7** with excess of pyrazole in the presence of CuI and potassium carbonate (nitrobenzene, T = 210 °C) afforded 1,4-bis(1-pyrazol-1*H*-yl)-benzene **8** in a high yield (76%). Subsequent iodination reaction was carried out using a mixture of **8**, iodic acid, and iodine. The reactants were heated at 80 °C in acetic acid and let to react for

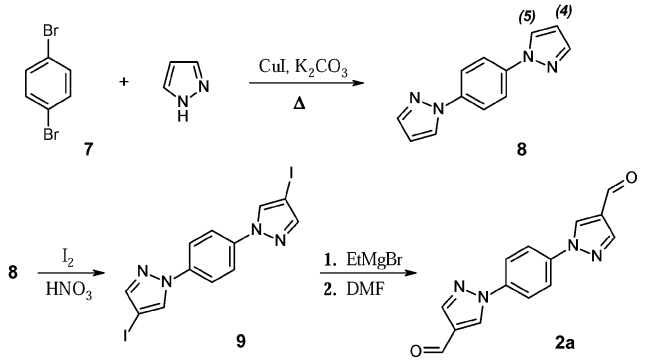

Scheme 2 Synthetic route towards dialdehyde **2a**.

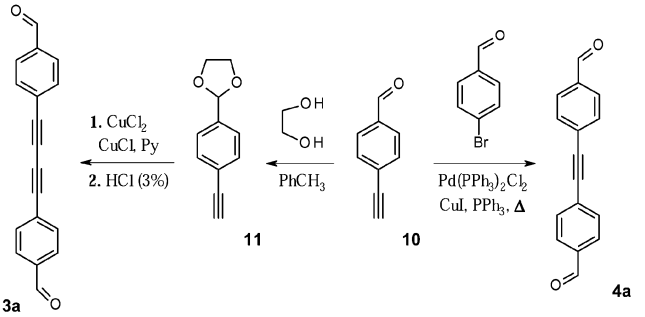

Scheme 3 Synthetic route towards dialdehydes **3a** and **4a**.

three days. The process progress was monitored by TLC and FD-mass analysis of the reaction mixture aliquots. Crude product precipitated upon cooling as colourless plates. Although the reaction yield appeared initially very good, the crude contained not only the target di-iodo derivative **9**, but also substantial amount of mono-iodinated species (~25%). Extension of the reaction time did not significantly improve the ratio between mono- and di-iodo derivatives. However, the mono-iodinated compound could be easily separated from the mother solution by filtration, leading to the di-iodinated compound **9** in fairly good yield (~60%). Notably, the mono-iodinated compound could be used itself as a starting material, in order to force the completion of the iodinating reaction, in other words, to functionalize the position 4 of the left unsubstituted pyrazole ring. Here, the disappearance of the pyrazole proton signal at 4^{th} position (6.50 ppm), is accompanied by a significant down-shift of the H signal at the 5^{th} position, from 7.75 ppm to 8.76 ppm in ^{1}H NMR spectra, and those resonances can be used as fingerprints to probe the progresses of conversion into compound **9**.

The final step towards dialdehyde **2a**, containing pyrazole-phenyl bridging unit, was accomplished *via* formylation reaction of the di-iodo derivative **9** through initial formation of the corresponding Grignard reagent. Compound **9** reacted smoothly with ethylmagnesium bromide. The magnesium intermediate was quenched with the stoichiometric amounts of DMF and afforded the target dialdehyde **2a** in high yield (89%).

The diacetylene fragment was introduced as the spacer into the π-system, giving rise to the biradical **3c** (class (ii)). It is expected that **3c** should feature little or no torsion within the molecule, which is essential for the weak *intra*-molecular coupling. One of the most efficient methods for the assembly of the molecules containing acetylene fragments relies on Glaser homo-coupling.[14] Regardless of the different coupling conditions tested, we could achieve only traces amounts of the dialdehyde **3a** employing direct Glaser coupling methodology to 4-ethynylbenzaldehyde **10** (Scheme 3). Thus, another route was undertaken, where the aldehyde function was at first protected with ethylene glycol affording the acetal precursor **11**.[15] The ^{1}H NMR spectrum of **11** showed characteristic signals of dioxolane ring at 4.0 ppm (–CH_3, methylene groups) and at 6.7 ppm (–CH). The signal associated to the aldehyde group, on the contrary, was absent, hence ensuring the complete conversion into the aldehyde-protected intermediate. The dioxolane derivative **11** was subjected to Glaser coupling. The reaction required excess of copper (I) and (II) chlorides (7 eq. and 5 eq., respectively) in pyridine media, followed by acidic cleavage of the dioxolane ring in THF–water mixture (5 : 3). Here, appearance in the ^{1}H, ^{13}C NMR spectra of strong signals typical for the aldehyde fragments at 10.0 (^{1}H) and 191 (^{13}C) ppm, confirmed successful completion of the coupling reaction and formation of the desired 4,4′-(buta-1,3-diyne-1,4-diyl)dibenzaldehyde **3a**.

To explore the potential of another closely associated derivative, the tolane dialdehyde **4a** was synthesized *via* Sonogashira–Hagihara cross-coupling reaction.[16] This system contains a shorter π-conjugated linker between the radical centres, hence the resulting through-bond exchange interaction is expected to be stronger in comparison to **3a**. The cross-coupling reaction between 4-bromobenzaldehyde and 4-ethynylbenzaldehyde **10** was carried out employing catalytic mixture of $Pd(PPh_3)_2Cl_2$, CuI, PPh_3 in the presence of base (Et_3N) and led to the formation of the dialdehyde **4a** in high yield (70%).

The target nitronyl nitroxide molecules could be routinely prepared as illustrated in Scheme 4. The condensation of the 2,3-diamino-*N*,*N*′-dihydroxy-2,3-dimethylbutane with carbaldehydes is an air-sensitive process and required, therefore, strict anaerobic conditions and degassed solvents.

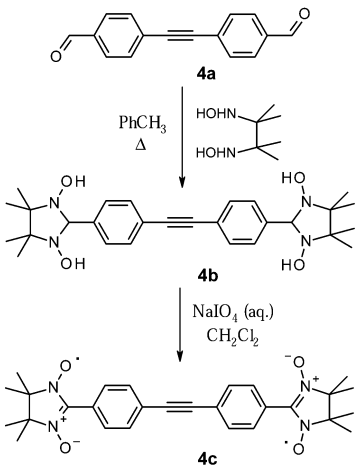

Scheme 4 Synthesis of the imidazolidine **4b** and biradical **4c**.

As a general rule, reaction with dialdehydes **1–4a** was performed in deaerated toluene under argon at 110 °C, and afforded the corresponding *N*,*N*′-dihydroxyimidazolidines **1b–4b** in quantitative yields. Once formed, the radical precursors (*e.g.* **4b** in Scheme 4) precipitated during the condensation step, and they were isolated by filtration as analytically pure (from ^{1}H-NMR spectra) white or yellowish powders. The ^{1}H-NMR spectra of these intermediates exhibited characteristic peaks of the hydroxy groups (~7.8–8.0 ppm, marked with the letter a in Fig. 2.) and the nodal proton located at the second position of the imidazolidine ring (~4.7 ppm, –CH group, labelled with the letter d). To illustrate this, the ^{1}H NMR spectrum of the condensation product **4b** is represented in Fig. 2. Here, the remaining in the sample toluene is specified with an asterisk.

Oxidation of the *N*,*N*′-dihydroxyimidazolidines **1b–4b** with sodium periodate in a biphasic media of dichloromethane and water afforded nitronyl biradicals **1c–4c** (Scheme 4). In order to avoid both further oxidation of the radicals to imino nitroxides, and to diminish the loss of the radical units, the reactions were carried out at T = 0–5 °C using an ice bath. This method was preferred over the one, where solid metal oxides were applied as oxidizing agents,[17,18] because it allowed a better control of the oxidation reaction by using stoichiometric amounts of periodate in solution. The progress of the reaction was monitored by TLC of the reaction mixture aliquots. All the radicals were purified using flash column chromatography on silica (SiO_2).

The synthesized nitroxide systems **1c–4c** were found fairly well soluble in most of the organic solvents tested (*e.g.* MeOH, $CHCl_3$, THF). However, in aprotic media (*e.g.* toluene), longer stability of the radical molecules over the time was observed. In protic solvents (*e.g.* CH_2Cl_2 or $CHCl_3$), partial decomposition of the radicals into diamagnetic products occurred within a day, due to sequential release of water molecules (dehydration), as witnessed from the decrease of the radical signal intensity in both UV-Vis absorption and in the EPR spectra (UV-Vis spectroscopy with absorption signals around 600 nm, and EPR resonance signals around g_{iso} = 2.0063).

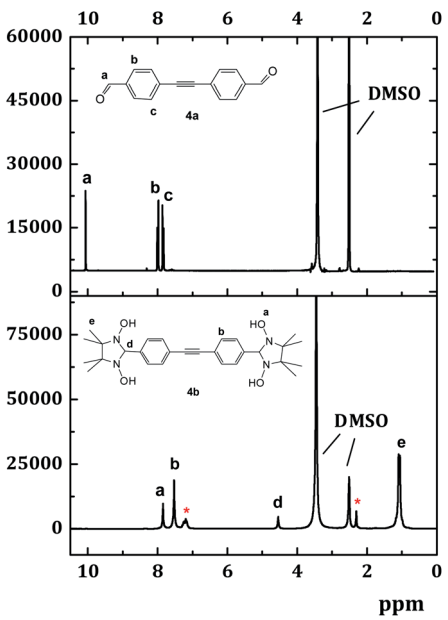

Fig. 2 NMR spectrum of **4a**, **b** in DMSO at 250 MHz (128 and 105 scans, respectively). The intensities of the solvent signals differ so much due to the significantly lower solubility of the dialdehyde **4a** in DMSO. The asterisk indicates toluene.

Absorption spectra (UV-Vis and IR spectroscopic studies)

The relevant UV-Vis and IR data recorded for **1c–4c** are given together in Table 1 for a better comparison.

The UV-Vis absorption spectra of the biradicals systems **1c–4c** were recorded in toluene solutions and exhibited the characteristic deep blue colour, which is typical for this class of radicals. Two distinctive set of absorption bands dominate the optical spectra (see ESI Fig. S1†). The first set of bands is characterized by differently enhanced vibronic components, and takes place at a longer wavelength, around 600 nm. Those signals correspond to the n–π* transitions of the aminoxyl oxides moiety. The second set of absorption values includes the π–π* transitions of the aromatic systems, and falls at much higher energy in the 300–380 nm range. Complementary to UV-Vis, the appearance of a novel signal after oxidation of the imidazolidine derivatives at around υ ~1350 cm^{-1} (Table 1) was assumed to arise from the N–O stretching vibration of the imidazoline moiety, which was in harmony with comparable signals observed for several other NN systems described in the literature.[19,20] Other strong signals appear at ~1550 cm^{-1}, but those are less characteristic since they belong to the C=N stretching vibrations. In addition, the IR spectra ensured absence of the traces of the dialdehyde precursors or imidazolidine condensation products in the purified biradical powders (see for comparison Fig. S2 and S3†).

EPR spectroscopy

The solution EPR spectra of the biradical systems **1c–4c** were recorded in oxygen-free toluene solutions (see ESI Fig. S4–S7†). at room temperature (T = 298 K). The nine lines splitting pattern witnessed in the studied systems highlights efficient through-bond coupling of the two nitronyl nitroxide residues *via* spin-polarization effects of the π-spacer. Regardless of the different distances between the radical centres, as well as in the molecular identity of the coupling units employed, this property hold for **1c**, **2c** and **4c**. Thus, within the limit of X-band EPR spectroscopy, the attainment of strong exchange interactions (J) $|J/a_N| \gg 1$ between the spin carriers were experimentally verified in all studied biradical systems. The spin-concentrations for **1c–4c** at T = 298 K were always consistent with two spin centres, where singlet and triplet states are thermally populated and statistically distributed according to the Boltzmann law. The calculated values of the hyperfine coupling constants (a_N) for **1c–4c** are given in Table 1 and fall between 0.7 and 0.8 mT ($g_{iso} \approx$ 2.0063). These values are in harmony with those typically observed in the nitronyl nitroxide radical systems found in the literature.

Table 1 Selected spectroscopic data for the nitronyl nitroxides **1c–4c**

Biradical	IR[a] ν_{NO}/cm^{-1}	UV-Vis[b] λ_{max} nm^{-1} (ε^b M^{-1} cm^{-1})	Mass[c] g mol^{-1}	EPR a_N/mT
1c	1358	627 (557)	599	0.752
2c	1354	599 (3808), 654 (4011)	519	0.768
3c	1365	622 (578)	511	0.744
4c	1356,1364	611 (868)	487	0.762

[a] Measured in solid state at room temperature ($T = 293$ K). [b] Measured in toluene solution except for compound **2c** that was measured in freshly prepared $CHCl_3$ solution. [c] Measured in dichloromethane by FAB. The m/z^+ (100%) peak corresponds to $[M]^+$.

Crystal structures analysis

Single-crystals suitable for X-ray analysis were obtained by slow diffusion of dichloromethane–hexane mixture (1 : 4) for biradicals **1c**, **3c** and **4c** at room temperature. Deep-blue needle crystals of biradicals **1c**, **3c** and **4c** were analysed by X-ray diffraction and their ORTEP drawing as given in Fig. 3–5. Pertinent crystallographic parameters and refinement data are listed in Table 2, while selected torsional angles for the studied biradicals are reported in Table 3.

As shown in the ORTEP diagram (Fig. 3), radical **1c** is symmetric to the central phenyl ring and has C_2 symmetry axis through C1–C4 atoms of the benzene ring. The dihedral angles between the phenyl ring and radical plane are 11.2° (N11···C17···C14···C13) and 5.75° (N12···C17···C14···C15). The O–N–C–N–O moiety is planar, with nearly equivalent O–N bond lengths of 1.31(O11···N11), 1.33 (O12···N12), 1.26 (O31···N31), 1.24 (O32···N32) Å. Closer analysis of the crystal packing shows that the N–O entities of neighboring molecules are attached to the benzene ring (O11···H161* 2.48, O12···H51* 2.6, O12···C36* 3.18 Å) and methoxy group of phenyl moiety to a radical fragment of the neighboring unit (O32···O1* 2.94, O32···C7* 3.02 Å); the shortest intersheet contact is found between the nitronyl oxygen and methyl group (O312···H203* 2.36 Å). Therefore, the intermolecular distances are short enough to favour magnetic interactions.

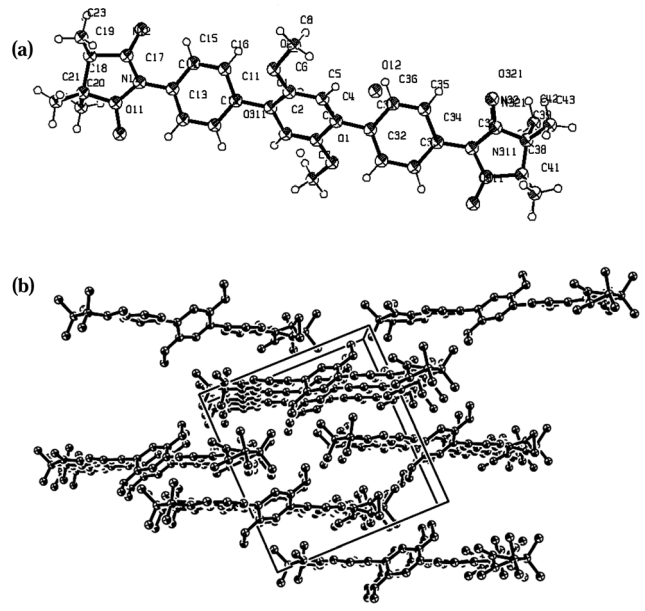

Fig. 3 X-ray structure and the crystal packing of **1c** with ORTEP drawn at the 50% of the probability level: (a) molecule; (b) crystal packing.

Table 2 Selected structural data for the biradicals **1c**, **3c** and **4c**

	1c	**3c**	**4c**
Formula	$C_{34}H_{40}N_4O_6$	$C_{30}H_{32}N_4O_4$	$C_{28}H_{32}N_4O_4$
M	600	512	488
Crystal system	Monoclinic	Monoclinic	Monoclinic
Space group	*Pn* (no. 7)	$P2_1/c$ (no. 14)	$P2_1/n$ (no. 14)
a/Å	13.045(5)	8.1768(2)	6.0834(4)
b/Å	8.447(4)	19.0191(8)	11.2581(5)
c/Å	13.703(5)	8.6983(3)	19.1236(9)
β/deg	91.593(12)	103.4(2)	90.832(3)
V/Å^3	1509.3(11)	1315.89(8)	1309.59(12)
Z	4	4	4
R_{factor}(%)	9.41	7.32	4.53
ρ_c/g × cm^{-3}	1.322	1.294	1.239
Mo kα/mm^{-1}	0.711	0.711	0.711
N_{ref}	4156	3687	3784
N_{par}	193	173	163
S	5.633	0.985	1.081
CCDC	822066	816633	816635

Table 3 Selected torsion angles Θ and bond lengths *d* for nitronyl nitroxide biradicals **1c**, **3c** and **4c**

	Biradical	d^a Å^{-1}	Θ^b/deg
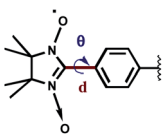	**1c**	1.443	27.5 ± 1
	3c	1.460	25.0 ± 1
	4c	1.459	24.4 ± 1

[a] Distance values were averaged (error within 0.002 Å). [b] Angle values were averaged (error within 1°).

The crystallographic data were collected on Nonius Kappa CCD (Mo kα, $\mu = 0.71073$ Å) diffractometer equipped with a graphite monochromator.

Compound **3c** is crystallized in a transoid arrangement with a center of symmetry located on the central C1–C1* bond (Fig. 4). The derivative is fairly planar, and there is a dihedral angle between the mean plane of the C6 ring and the imidazolidine moiety of 25°. In the present structure the distances between the N–O and C–N atoms of the radical subunits are

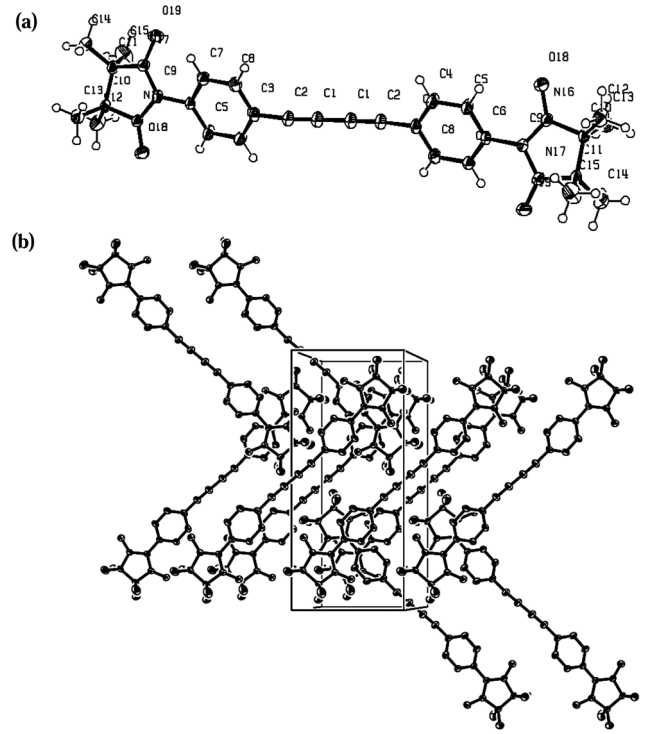

Fig. 4 X-ray structure and the crystal packing of **3c** with ORTEP drawn at the 50% of the probability level: (a) molecule; (b) crystal packing. View along the **c** axe of the crystal packing of compound **3c**.

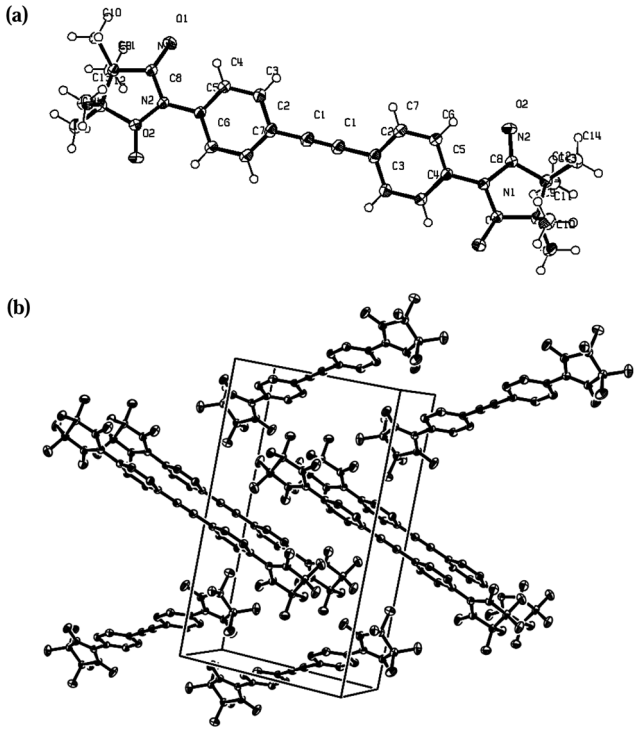

Fig. 5 X-ray structure of **4c** with ORTEP drawn at the 50% of the probability level: (a) molecule; (b) crystal packing.

similar: N(16)–O(18) 1.276; N(17)–O(19) 1.281; N(16)–C(9) 1.36; N(17)–C(9) 1.345 Å. This symmetry is due to the complete delocalization of the odd electron in the non-bonding orbitals of the 'ONCNO' core. The N–O bond and the C–N bond distances are between the values of a single and a double bond. Closer examination of the crystal packing shows that the radicals are organized in a zig-zag fashion (O18···H133* 2.53 Å, Fig. 4(b)) with additional hydrogen bonds between the sheets formed by C5 atom of the benzene ring with hydrogen atoms (C5···H71* 2.8, C5···H152* 2.86 Å, Fig. 4).

The molecular structure of compound **4c** (Fig. 5) is similar to the one previously reported[21] which has the same space group ($P2_1/n$). Probably, such similar cell organization can be explained by crystallization conditions. The torsion angle between the plane of the benzene ring and the radical moiety is 25°. Adjacent radicals are organized in a head-to-tail fashion forming 1D network: the first N–O fragment of each radical unit is attached to C7, H71 atoms of the benzene ring, the second NO binds to the hydrogen atoms of the methyl group of an imidazolidine fragment. Geometrical parameters are: O2···H71* 2.52, O1···H141* 2.59, O2···C7* 3.16, C7···C13 3.4 Å; the distance between H-bonded sheets totals 2.36 Å (O1···H101*).

Reasonably to assume, that the intermolecular interaction in two radicals oriented in a head-to-tail fashion is at maximum when the two NO groups are arranged in such a way that the O–N···O* angle α is equal to 90° and the angle β between the π* orbitals of the nitronyl nitroxide radicals with a vector normal to the N2O2 plane is also 90°.[22,23] Thus, not only the intermolecular distances but the whole molecular structure of the biradical **4c** favours intermolecular magnetic interactions.

In order to rationalize the magnetic properties of molecular compounds, analysis of the molecular packing (so, as to find out the possible magneto-structural correlations) was carried out. The studied biradical NN systems shared nearly planar arrangements of the coupling-core. Structural analyses revealed rather small torsions between the imidazolyl and the aromatic core (<30°), which facilitates efficient communication between the radical moieties through the coupler. Additionally, the intersheet contacts are found to be short enough (~2.5 Å) to favour magnetic interactions.

DFT calculations and magnetic measurements

In order to understand the influence of the bridging unit on the electronic properties and especially on the exchange coupling, DFT calculations were performed. We thus carried out a geometry optimization with the B3LYP hybrid function and 6-31G* basis set and we then applied the broken symmetry approach (BS) for the singlet and triplet states with BLYP (to avoid Hartree–Fock contamination) and 6-31G* basis set according to an approximate projection technique as suggested by Yamaguchi.[24] For the simplest case of two spins $S = 1/2$ this form of the spin Hamiltonian ($H = -2J_{12}S_1S_2$, here the exchange parameter J will be negative in the case of antiferromagnetic interaction) gives the exchange interaction as $J = (E(\mathrm{BS}) - E(T))/(S^2(T) - S^2(\mathrm{BS}))$, where E(BS) is the energy of the broken symmetry approach, $E(T)$ is the energy of the triplet state and S^2 are the eigenvalues of the spin operator for these states. In case

Table 4 The *intra*-dimer magnetic exchange coupling calculated J_{calc} and experimental constant J_{exp} values. T_{max} denotes the position of the maximum in $\chi_{mol}(T)$

Biradical	T_{max}/K	J_{calc}/K[a]	J_{calc}/K[b]	J_{exp}/K[c]
1c	0.7	−2.7	−2.0	−0.9
2c	19.5	−2.5	—	−16.0!
3c	3.2	−14.4	−5.8	−2.4
4c	6.3	−16.8	−8.6	−4.8

[a] Optimized geometries were obtained from DFT calculations (B3LYP, 6-31G*), then the broken symmetry approach was applied (BLYP, 6-31G*) for the evaluation of J. [b] The exchange interactions were evaluated for X-ray crystal structures applying the broken symmetry approach with BLYP functionals and 6-31G* basis set. [c] Expected from the isolated dimer model, where $2J/k_BT_{max} = 1.599$.

of weak interaction without spin contamination $S^2(T) = 2$ and $S^2(BS) = 1$ the direct exchange yields $J = E(BS) - E(T)$. The obtained theoretical exchange coupling constants J are listed in Table 4 together with the experimental values for a better comparison.

The magnetic properties of the samples **1c–4c** were determined in the temperature range 2 K ≤ T ≤ 270 K and in magnetic fields $B \leq 5$ T by using a Quantum Design SQUID magnetometer. All data have been corrected for the temperature-independent diamagnetic core contribution of the constituents[25] and the magnetic contribution of the sample holder. For temperatures below 2 K the ac-susceptibility data shown in Fig. 7 were recorded using an ultra-high resolution ac-susceptometer adapted to a ^{3}He–^{4}He top-loading dilution refrigerator. The compensated-coil susceptometer is optimized for measuring small single crystals in the mg range. The system is equipped with a 12 T superconducting magnet.

Generally, all the biradicals under investigation (**1c–4c**) featured a similar magnetic behaviour in the studied temperature range. The high-quality single crystalline materials **1c**, **3c**, and **4c** exhibit magnetic contributions of Curie type, assigned to uncoupled spins, the concentration of which is much less than 1%. The Curie contribution for the biradical **2c** was slightly larger. Furthermore the small Curie contribution for **2c** is indicated by the broken line in the inset of Fig. S9.†

As an example for the magnetic behaviour of the biradicals **1c–4c**, we show the magnetic susceptibility, plotted as $\chi_{mol}T$, for the system **4c** in Fig. 6. The data reveal an almost temperature-independent behaviour in the range from about 100 K to 270 K, with a value $\chi_{mol}T = (0.734 \pm 0.005)$ cm^3 Kmol^{-1}. This value is very close to the theoretically expected value of 0.75 cm^3 Kmol^{-1} for two independent spin $S = 1/2$ entities (broken line in Fig. 6). Very similar values of $\chi_{mol}T = (0.731 \pm 0.017)$ cm^3 Kmol^{-1} were observed for the biradicals **1c–3c** in the same temperature range. On cooling $\chi_{mol}T$ becomes progressively reduced below about 140 K, a clear signature of dominant antiferromagnetic through-bond interactions between radical centers (*intra*-dimer coupling). An estimate of the mean value for the magnetic exchange coupling in the high-temperature regime can be obtained by fitting the inverse magnetic susceptibility $1/\chi_{mol}$ by a Curie–Weiss model in the temperature range 70K ≤ T ≤ 270

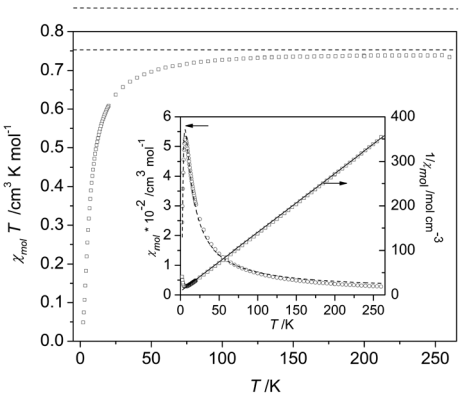

Fig. 6 Magnetic susceptibility in a representation $\chi_{mol}T$ of biradical **4c**. The broken line indicates the theoretical value of 0.75 cm^3 K mol^{-1} for a dimer system formed by two spin $S = 1/2$ entities. Inset: molar susceptibility χ_{mol} (left scale) and its inverse $1/\chi_{mol}$ (right scale) as a function of temperature together with fits performed by using a Curie–Weiss expression (solid line) and a Bleaney–Bowers equation[26] (broken line). For fitting parameter and details see text.

K, *cf.* straight line in the inset of Fig. 6. The fit yields an antiferromagnetic Weiss temperature $\theta_W = -(8.2 \pm 0.5)$ K. For a more precise determination of the dominant magnetic interactions, the temperature dependence of the molar magnetic susceptibility over the whole temperature range 2 K ≤ T ≤ 270 K was fitted using the Bleaney–Bowers equation[26] for isolated dimers, *cf.* inset to Fig. 6. The *intra*-dimer magnetic exchange coupling constant J_{intra} between two $S = 1/2$ spins used in this expression refers to a Hamiltonian of the form $H = -2J_{12}S_1S_2$, which was taken also for the DFT calculations. The inset of Fig. 6 demonstrates that the isolated-dimer model provides a reasonable description of the overall behaviour of $\chi_{mol}(T)$ for the biradical **4c**. The biradicals **1c** and **3c** exhibited a similar behaviour, in accordance with the theoretical prediction, and their $\chi_{mol}(T)$ data were analyzed by an analogous procedure. Their *intra*-dimer exchange constants are listed in Table 4.

However, a closer inspection of the low-temperature (T < 4 K) susceptibility data as a function of temperature, and at T = const. as a function of magnetic field, for the various biradicals (see Fig. 7 below for **4c**) revealed significant deviations from the

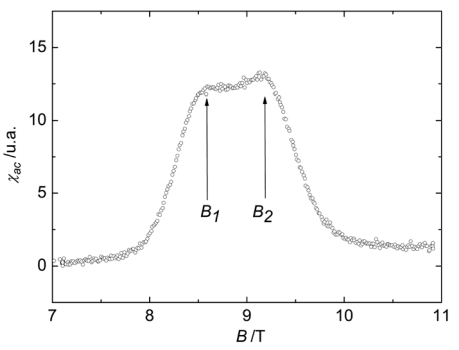

Fig. 7 AC-susceptibility of the biradical **4c** at T = 191 mK. The data feature rounded peaks at $B_1 \approx 8.6$ T and $B_2 \approx 9.2$ T.

isolated-dimer model. These deviations were attributed to the small magnetic *intra-* and *inter*-molecular interactions between neighboring biradicals mediated *via* hydrogen bonds (**1c**, **3c**, **4c**). The strength of these interactions depends on the distance and relative orientation of the biradicals.[27–29]

The results of AC-susceptibility measurements as a function of magnetic field at a constant temperature of 191 mK are shown in Fig. 7 on example of biradical **4c**. The rounded double-peak structure in the data, with the peak positions $B_1 \approx 8.6$ T and $B_2 \approx 9.2$ T, indicates a field-induced magnetic state for $B_1 \leq B \leq B_2$. Note that B_2 roughly corresponds to the saturation field B_s. Similar anomalies in the susceptibility are found in other spin ladder compounds, like $(C_5H_{12}N)_2CuBr_4$,[30] which represent a class of low-dimensional materials with structural and physical properties lying between those of 1D and 2D systems. While a rounded double-peak structure is expected when the *inter*-dimer couplings are one- or quasi two- dimensional, sharp peaks reflect three-dimensional interactions. In fact, a quasi two-dimensional magnetic behaviour for the biradical **4c** is also suggested by its crystal structure.

In leading order, the fields B_1 and B_2 ($\approx B_s$) are related to the dominant J_{intra} and an averaged J_{inter} by $g\mu_B B_1/2 = J_{\mathrm{intra}} - (J_{\mathrm{inter}})_{\mathrm{aver}}$ and $g\mu_B B_2/2 = J_{\mathrm{intra}} + 2(J_{\mathrm{inter}})_{\mathrm{aver}}$ (see, *e.g.* ref. 30 and references cited therein), resulting in $(J_{\mathrm{inter}})_{\mathrm{aver}}$ of the order of -1 to -2 K for **4c**. These are typical values for magnetic interactions mediated by hydrogen bridges.[27–29] Thus, according to our magnetic characterization, the nitronyl biradical **4c** is a promising candidate for a purely organic-based quasi two-dimensional quantum magnet.

Remarkably, the biradical **2c** shows significant deviations from the theoretical expectation, *cf.* Table 4. For this system the maximum of χ_{mol} was located at a temperature $T_{\max} = 19.5$ K, distinctly higher than expected from DFT calculations for an isolated single biradical entity. This is different for all other biradicals shown in Table 4 where the agreement between experimental value and theoretical prediction is reasonably good. This might be the result of a peculiar magneto-structural correlation influence and/or strong *inter*-molecular exchange interactions existing in the material **2c**. For instance, attraction of a neighboring radical to the lone pair of the nitrogen atom of the pyrazolyl moiety in **2c** or stronger orbital overlap between the radical centres might cause such a drastic change in the magnetic properties of this biradical. In fact, the magnetic interactions based on structural peculiarities of this type are difficult to predict. The strength of these interactions strongly depends on the relative geometry between the interacting magnetic orbitals which is also determined by the crystal packing. Better understanding of the origin of such an unexpected behaviour in **2c** therefore requires a detailed analysis of the crystal structure. Work on obtaining a suitable crystal for X-ray measurement is in progress.

Conclusions

In this study a series of novel nitronyl nitroxide biradicals **1c–4c** coupled *via* modified tolane linkers was synthesized and their magnetic behaviour was studied. The tolane bridge seemed to be perfectly suited for the requirement of *intra*-dimer exchange coupling $J \sim 10$ K. The structural analyses showed that the small torsions between the radical moieties and the modified diacetylene bridging subunit assist unimpeded through-bond exchange, as well as the small intersheet distances (π-stacking) favour efficient magnetic interactions. Magnetic measurements and their interpretation revealed that the biradical **2c** exhibits surprisingly strong antiferromagnetic interactions, much larger than predicted for *intra*-molecular exchange interaction. In all other cases weak through-space antiferromagnetic interactions are predominant.

Summarizing, we found promising candidates for the quest to synthesize a purely organic molecular magnet. Quantum Monte Carlo simulations for analysing the low-temperature susceptibility data are underway in order to derive the underlying effective exchange coupling topology of this compound. Efforts towards the preparation of extended networks through the formation of complexes with different metal ions coordinated to the radical unit and/or π-bridge are presently on-going. It would be of interest to extend these studies to other series of tolane-bridged biradicals, in particular the idea to introduce additional chelating sites within the core is considered.

Experimental

General Remarks

All chemicals and reagents were used as received from commercial sources (Acros Organics, Aldrich, Fluka, Lancaster, Merck and Strem) without additional purification. Solvents for synthesis were used as received, unless otherwise mentioned. ESR spectra were recorded in dilute, oxygen-free solutions in toluene, concentration $\sim 10^{-4}$ mol L, using a Bruker X-band spectrometer ESP300 E, equipped with an NMR gaussmeter (Bruker ER035), a frequency counter (Bruker ER041XK) and a variable temperature control continuous flow N_2 cryostat (Bruker B-VT 2000). The *g*-factor corrections were obtained using the DPPH ($g = 2.0037$) as standard. UV-Vis spectra were recorded in toluene solutions with a Perkin-Elmer spectrometer (UV/Vis/NIR Lambda 900) using a 1 cm optical path quartz cell at room temperature, unless otherwise specified. ^{1}H and ^{13}C NMR spectra were recorded on a Bruker DPX 250, Bruker DMX 300 spectrometer. Solid powders were pressed and IR spectra of the samples were recorded as they were (Nicolet 730 FT-IR spectrometer). Mass spectra were obtained on FDMS, VG Instruments ZAB-2 mass spectrometer. Elemental analyses were performed at the University of Mainz, Faculty of Chemistry and Pharmacy on a Foss Heraeus Varieo EL. The melting points were measured on a Büchi B-545 apparatus (uncorrected) by using open-ended capillaries.ESI.†

2,3-Dimethyl-2,3-bis(hydroxylamino)butane (BHA). A mixture of 17.6 g 2,3-dimethyl-2,3-dinitrobutane and 27.0 g of Zn (dust) in 300 mL THF and 50 mL H_2O was cooled down to 0–5 °C in an ice bath. Keeping this temperature constant solution of 43 g NH_4Cl in 150 mL H_2O was added dropwise under vigorous (mechanical) stirring. After addition was completed (*ca.* 2.5 h) the reaction was stirred for 1.5 h at the same temperature, and an additional 0.5 h at room temperature. The

white-gray precipitate of Zn slurry was filtered off, and was washed with THF (4 × 20 mL). Filtrate was evaporated to viscous residue, cooled to −15 °C (the mixture was kept in the freezer for 1 h). After that the flask was filled with argon and a mixture of 50 g Na_2CO_3 and 30 g NaCl salts was added at once. The flask was shaken for 15 min, and after homogenization the white solid was charged into a Soxhlet apparatus, protected from air (argon balloon) and extracted with 300 mL of dichloromethane (72 h). White precipitate was filtered off, washed with dichloromethane (2 × 15 mL), hexane (2 × 10 mL) and dried on air. Yield is 6.1 g (42%). M p 160–161 °C. IR (powder, ν/cm^{-1}): 3257 (*vs.* and broad, ν_{OH}), 2987 (*vs.*, ν_{C-H}), 1479–1374 (*vs.*, several bands), 1261 (s), 1178 (*vs.*), 1145 (*vs.*), 1080 (s), 1035 (*vs.*), 989 (m), 952 (*vs.*), 904 (*vs.*), 852 (m), 790 (m), 690 (m).

A. General procedure of the condensation reaction between 2,3-dimethyl-2,3-bis(hydroxylamino)butane with aldehydes. A suspension of BHA (1.1 eq. for each aldehyde group) and an aldehyde (1.0 eq.) in toluene (5 mL mmol^{-1}) was carefully deaerated using argon bubbling for ~20 minutes. The flask was provided with a condenser containing an argon balloon, and moved into an oil bath. The mixture was heated under argon near reflux for 2–18 h. The progress of the reaction was monitored by TLC (SiO_2, hexane/ethyl acetate or dichloromethane with 5% of methanol). After the process was completed and the flask was cooled down till room temperature formed precipitate (white or yellowish) was filtered off, washed with toluene (2 × 10 mL), heptane (1 × 10 mL) and dried on air. The product was used for the next step without additional purification.

B. General procedure for oxidation of 4,4,5,5-tetramethylimidazolidine-1,3-diol derivatives to nitronyl nitroxides. A suspension of 4,4,5,5-tetramethylimidazolidine-1,3-diol (1 mmol) in H_2O–CH_2Cl_2 (1 : 2) mixture (~50 mL) was cooled down to 0–5°C (to avoid overoxidation and formation of imino nitroxide species) using an ice bath. To that mixture $NaIO_4$ 5% aqueous solution (0.8 eq.) was added dropwise. After reaction was complete (0.5–3 h), dark-blue organic layer was separated. The aqua phase was extracted with dichloromethane (3 × 25 mL). The combined organic extracts were additionally washed with water (2 × 30 mL), NaCl saturated aqueous solution (1 × 50 mL), dried over $MgSO_4$ (in some cases – Na_2SO_4). The residue after filtration was evaporated and purified using a chromatographic column (SiO_2, hexane/ethyl acetate or CH_2Cl_2/MeOH).

2,5-Dimethoxy-1,4-phenyldiboronic acid 6.[31] To a solution of 1,4-dibromo-1,5-dimethoxybenzene **5** (2.96 g, 10.0 mmol) in dry THF (100 mL) *n*-BuLi (13.3 mL, 21.25 mmol, of 1.6 M in hexane) was added dropwise in 30 minutes at −78 °C. The mixture was stirred during 5 h with cooling, and B(O*i*-Pr)$_3$ (10 mL, 43.4 mmol) was added slowly keeping the temperature constantly at −78 °C. The resulted solution was stirred overnight and allowed to warm slowly to room temperature. The mixture was decomposed with 5% HCl (20 mL) and THF was removed *in vacuo*. White crystalline residue was filtered off and washed with large amount of water. Compound **6** was recrystallized from H_2O–CH_3CN (1 : 1, 100 mL) mixture, affording white needles of the product **6** in 45% yield (1.02 g). ^{1}H-NMR ($(CD_3)_2SO$, 250 MHz, 298 K, 16 scan), δ ppm: 3.78 (s, 6H, –OCH_3), 7.16 (s, 2H, Ar-H), 7.82 (s, 4H, –B(OH)$_2$). ^{13}C-NMR ($(CD_3)_2SO$, 63 MHz, 298K, 256 scan), δ ppm: 55.6, 116.8, 124.6, 157.4. FAB$^+$ *m*/*z* 225.9 [M]$^+$.

4-[4-(4-Formylmethyl)-2,5-dimethoxyphenyl]benzaldehyde 1a (ref. 32). A mixture of 2,5-dimethoxy-1,4-phenylenediboronic acid **6** (0.76 g, 3.40 mmol), 4-bromobenzaldehyde (1.24 g, 6.68 mmol), K_2CO_3 (23 g), H_2O (10 mL) and THF (75 mL) was degassed using argon bubbling for 30 min. After that the mixture was heated to 80 °C and solution of Pd(PPh$_3$)$_4$ (0.19 g, 0.167 mmol) in THF (5 mL) was added through the rubber septum. Light yellow mixture was stirred under reflux for 120 h. The solvent was removed, residue was mixed with 500 mL of H_2O and stored in fridge for 24 h. Light yellow needles were filtered off, washed with EtOH–H_2O (1 : 1) mixture and dried (0.71 g, 62%). ^{1}H-NMR ($(CD_3)_2SO$, 250 MHz, 298 K, 64 scan), δ ppm: 3.80 (s, 6H, –OCH_3), 7.12 (s, Ar-H), 7.80, 7.95 (both dd, 4H, ^3J = 8.15 Hz, Ar-H), 10.04 (s, 2H, –CHO). ^{13}C-NMR ($(CD_3)_2SO$, 176 MHz, 323 K, 51200 scan), δ ppm: 56.4, 114.8, 129.2, 129.4, 130.0, 134.9, 143.8, 150.5, 192.7. FAB$^+$ *m*/*z* 346.52 [M]$^+$.

2-(4-{4-[4-(1,3-Dihydroxy-4,4,5,5-tetramethyl-imidazolidine-2-yl)phenyl]-2,5-dimethoxyphenyl}phenyl)-4,4,5,5-tetramethyl-imidazolidine-1,3-diol 1b. Compound **1b** was synthesized following the method **A** as slightly yellowish crystals in 97% yield (170 mg). ^{1}H-NMR ($(CD_3)_2SO$, 250 MHz, 298 K, 64 scan), δ ppm: 1.09, 1.11 (both s 12H, –CH_3), 3.77 (s, 6H, –OCH_3), 4.57 (s, 2H, –CH–), 7.01 (s, 2H, Ar-H), 7.53 (s, 8H, Ar-H), 7.80 (s, 4H, –N–OH). ^{13}C-NMR ($(CD_3)_2SO$, 63 MHz, 298 K, 256 scan), δ ppm: 17.3, 24.5, 56.2, 66.1, 90.2, 114.5, 128.3, 128.6, 129.7, 137.0, 140.8, 150.3. FAB$^+$ *m*/*z* 606.74 [M]$^+$.

2-(4-{4-[4-(1-Oxyl-3-oxo-4,4,5,5-tetramethyl-4*H*,5*H*-imidazolin-2-yl)phenyl]-2,5-dimethoxyphenyl}phenyl)-4,4,5,5-tetramethyl-imidazoline-1-oxyl-3-oxo 1c. Chromatography purification on silica gel with CH_2Cl_2–MeOH (30 : 1) eluent afforded dark-blue prisms of biradical **1c** in 54% yield (0.15 g). UV-Vis (toluene): λ/nm (ε/M^{-1} cm^{-1}) 627 (557), 356 (20425). (Calc. for $C_{34}H_{40}N_4O_6$: C, 67.98; H, 6.71; N, 9.33C. Found: C, 67.90; H, 6.66; N, 9.43%).

1-[4-(1*H*-pyrazol-1-yl)phenyl]-1*H*-pyrazole 8 (ref. 33). A mixture of 1,4-dibromobenzene **7** (2.37 g, 0.01 mol), pyrazole (6.71 g, 0.10 mol), CuI (4.95 g, 0.026 mol) and K_2CO_3 (16.58 g, 0.12 mol) in $PhNO_2$ (20 mL) was refluxing for 3 h. Solvent was removed *in vacuo*, and the residue was washed with CH_2Cl_2 (3 × 150 mL). Filtrate was evaporated on rotary and purified on a chromatographic column (SiO_2, CH_2Cl_2), giving after evaporation of the solvents 1.6 g of the colorless needles of compound **8** (76%). ^{1}H-NMR ($CDCl_3$, 250 MHz, 298 K, 64 scan), δ ppm: 6.50 (dd, 2H, J = 1.62, J = 2.39 Hz), 7.75 (d, 2H, J = 1.62 Hz), 7.80 (s, 4H, Ar-H), 7.95 (d, 2H, J = 2.39 Hz). ^{13}C-NMR ($CDCl_3$, 63 MHz, 298 K, 274 scan), δ ppm: 107.9, 120.0, 126.7, 138.4, 141.3. FAB$^+$ *m*/*z* 210.10 [M]$^+$.

4-Iodo-1-[4-(4-iodo-1*H*-pyrazol-1-yl)phenyl]-1*H*-pyrazole 9. A mixture of 1-[4-(1*H*-pyrazol-1-yl)phenyl]-1*H*-pyrazole **8** (1.47 g, 7.0 mmol) and 30% H_2SO_4 (2.5 mL) in conc. AcOH (20 mL) was heated up to 80 °C. To this mixture a solution of I_2 (1.42 g, 5.6 mmol), HIO_3 (0.49 g, 2.8 mmol) in AcOH (400 mL) and H_2SO_4 (2 mL) was added dropwise within 60 min. The resulted red-brown solution was heated for 60 h at the same temperature. During reaction colourless crystals were formed. Reaction mixture was cooled to ambient temperature, and sodium thiosulfate was

added until the solution became colourless. Crystalline solid was filtered off and washed with AcOH (3 × 5 mL), water (3 × 10 mL), $NaHCO_3$ saturated aqueous solution (3 × 5 mL), and EtOH (2 × 5 mL). Drying compound on air resulted in 1.9 g (59%) of the titled derivative **9** (in addition 0.62 g (26%) of monoiodo derivative was isolated from the filtrate). ^{1}H-NMR ($(CD_3)_2SO$, 250 MHz, 298 K, 64 scan), δ ppm: 7.86 (w. s, 2H), 7.95 (w. s, 4H, Ar-H), 8.76 (w. s, 2H). ^{13}C-NMR ($(CD_3)_2SO$, 63 MHz, 298 K, 256 scan), δ ppm: 101.7, 119.4, 132.2, 142.2, 145.9. FAB$^+$ *m*/*z* 462.03 $[M]^+$. (Calc. for $C_{12}H_8I_2N_4$: C, 31.19; H, 1.75; N, 12.13. Found: C, 31.08; H, 1.16; N, 12.03%).

4-Formyl-1-[4-(4-formyl-1*H*-pyrazol-1-yl)phenyl]-1*H*-pyrazole 2a. A suspension containing starting compound **9** (1.4 g, 3.03 mmol) in THF (50 mL) was subjected reaction with EtMgBr (6.3 mL, 6.36 mmol, 1 M in THF) under argon. The mixture was stirring at 60°C for 1 h, and then solution of dry DMF (0.5 mL, 6.36 mmol) in dry THF (1 mL) was added dropwise. Cold light yellow reaction mixture was decomposed with NH_4Cl saturated aqueous solution (20 mL). Excess of THF was evaporated, water residue was extracted with EtOAc (4 × 100 mL). The combined organic fractions were dried over Na_2SO_4, filtrated and solvent was removed *in vacuo*. Yellow precipitate was washed with hexane (3 × 15 mL) and dried on air. Obtained 0.71 g of dialdehyde **2a** (89%). ^{1}H-NMR ($(CD_3)_2SO$, 250 MHz, 298 K, 64 scan), δ ppm: 8.06 (w. s, 2H), 8.28 (w. s, 4H, Ar-H), 9.26 (w. s, 2H), 9.92 (w. s, 2H, –CHO). ^{13}C-NMR ($(CD_3)_2SO$, 63 MHz, 298K, 256 scan), δ ppm: 120.3, 125.6, 132.4, 137.6, 141.5, 184.9. FAB$^+$ *m*/*z* 266.28 $[M]^+$. (Calc. for $C_{14}H_{10}N_4O_2$: C, 63.15; H, 3.79; N, 21.04. Found: C, 63.18; H, 3.68; N, 21.13%).

2-(1-{4-[4-(1,3-Dihydroxy-tetramethyl-imidazolidine-2-yl)-1*H*-pyrazol-1-yl]phenyl}-1*H*-pyrazole-4-yl)-4,4,5,5-tetramethyl-imidazolidine-1,3-diol 2b. The condensation was realized using procedure **A**: starting from 0.2 g (0.75 mmol) of dialdehyde **2a** and 0.27 g of BHA (1.84 mmol) 0.34 g of the imidazolidine **2b** was obtained (87%). ^{1}H-NMR ($(CD_3)_2SO$, 250 MHz, 298 K, 64 scan), δ ppm: 1.06, 1.08 (both s 12H, $-CH_3$), 4.67 (s, 2H,–CH–), 7.71 (s, 2H), 7.81 (w. s, 4H, –NOH), 7.90 (s, 4H, Ar-H), 8.38 (s, 2H). ^{13}C-NMR ($(CD_3)_2SO$, 63 MHz, 298 K, 256 scan), δ ppm: 17.4, 23.9, 65.0, 83.1, 119.0, 125.4, 126.7, 137.5, 140.9. FAB$^+$ *m*/*z* 526.63 $[M]^+$.

2-(1-{4-[4-(1-Oxyl-3-oxo-4,4,5,5-tetramethyl-4*H*,5*H*-imidazolin-2-yl)-1*H*-pyrazol-1-yl]phenyl}-1*H*-pyrazole-4-yl)-4,4,5,5-tetramethyl-imidazoline-1-oxyl-3-oxo 2c. Compound **2c** was synthesized using methodology B from bisimidazolidine **2b** (0.50 g, 0.95 mmol) in good yield (0.30 g, 61%) as dark-blue fine needles: UV-Vis ($CHCl_3$): λ/nm (ε/M^{-1} cm^{-1}) 599 (3804), 654 (4011), 321 (69198), 366 (31143). FT-IR (powder, ν/cm^{-1}) 3179, 3164 (w, ν_{C-H}, aromatic), 2985, 2930 (m, ν_{C-H}), 1680 (s), 1601 (m, ν_{Ph}), 1528 (*vs.*), 1450 (m), 1425 (s), 1417 (s), 1400 (m), 1386 (*vs.*, ν_{methyl}), 1354 (*vs.*, ν_{NO}), 1332, 1314 (*vs.*, pyrazolyl-moiety), 814 (*vs.*, $\nu_{p\text{-}sub\text{-}Ph}$). (Calc. for $C_{26}H_{32}N_8O_4$: C, 59.99; H, 6.20; N, 21.52. Found: C, 60.18; H, 6.16; N, 21.34%).

2-(4-Ethynyl phenyl)-1,3-dioxolane 11. 4-Ethynylbenzaldehyde **10** (1.76 g, 13.53 mmol) was charged into a flask together with ethyleneglycol (1.4 mL, 25.15 mmol), *para*-toluene-sulfonic acid (0.2 g, 1 mmol) and toluene (60 mL). The solution was heated to reflux with Deane-Stark for one day. Then it was neutralized with $NaHCO_3$ aqueous solution and the phases were separated. The aqueous layer was extracted with small portions of toluene (3 × 10 mL) and the combined organic layers were collected, dried over $MgSO_4$ and filtrated. Toluene solution was evaporated under reduced pressure. Crude orange oil was purified using column chromatography (SiO_2, dichloromethane). Compound **11** was obtained as slightly yellow oil in 85% yield (2 g). ^{1}H-NMR ($CDCl_3$, 250 MHz, 298 K, 16 scan), δ ppm: 3.02 (s, 1H), 3.99 (m, 4H, -CH_2), 6.73 (s, 1H), 7.91 (dd, 4H, ^3J = 8 Hz, Ar-H). ^{13}C-NMR ($CDCl_3$, 63 MHz, 298K, 256 scan), δ ppm: 67.2, 82.4, 84.2, 103.9, 123.2, 127.2, 134.5, 137.8. FAB$^+$ *m*/*z* 173.0 $[M]^+$.

1,4-Bis(4-(1,3-dioxolan-2-yl)phenyl)buta-1,3-diyne 3. Glaser coupling.[14] A mixture of 2-(4 ethynyl phenyl)-1,3-dioxolane **11** (3.57 g, 20.52 mmol), CuCl (14 g, 141.4 mmol), $CuCl_2$ (14.3 g, 106.3 mmol) and dry pyridine (120 mL) was stirred at room temperature for 24 hours; then it was washed with 10% HCl (1 × 40 mL) and extracted with Et_2O (5 × 60 mL). The combined organic extracts were washed with NH_4Cl saturated solution (to remove excess of copper) and dried over $MgSO_4$. As the main product 1,4-bis(4-(1,3-dioxolan-2-yl)phenyl)buta-1,3-diyne **3** was isolated from the reaction mixture using column chromatography (SiO_2, dichloromethane) in 60% yield (4.26 g). ^{1}H-NMR ($CDCl_3$, 250 MHz, 298 K, 16 scan), δ ppm: 3.95 (m, 8H, $-CH_2$), 5.77 δ (s, 2H), 7.38 δ (d, 4H, ^3J = 8 Hz), 7.45 δ (d, 4H, ^3J = 8 Hz). ^{13}C-NMR ($CDCl_3$, 63 MHz, 298 K, 256 scan), δ ppm: 66.5, 73.3, 82.4, 103.1, 122.6, 126.8, 133.1, 138.9. FAB$^+$ *m*/*z* 346.2 $[M]^+$.

4,4′-(Buta-1,3-diyne-1,4-diyl)dibenzaldehyde 3a (ref. 34). Solution of **3** (1.78 g, 5.14 mmol) in THF (50 mL) was cooled to 5 °C using an ice bath, and 3% HCl (30 mL) was added. The mixture was stirred for 45 min the ice bath and additional 1 h at room temperature. After that THF was evaporated. The residue was diluted with Et_2O (60 mL), washed with water (3 × 35 mL) and dried over $MgSO_4$. Solvent was evaporated under reduced pressure. Dialdehyde **3a** was obtained as light yellow solid in 86% yield (1.15 g). ^{1}H-NMR ($(CD_3)_2SO$, 250 MHz, 298 K, 16 scan), δ ppm: 7.91 (d, 4H, ^3J = 8 Hz), 8.03 (d, 4H, ^3J = 8 Hz), 10.12 (s, 2H). ^{13}C-NMR ($(CD_3)_2SO$, 75 MHz, 353 K, 1801 scan), δ ppm: 75.8, 82.1, 125.5, 129.1, 132.7, 136.3, 191.7. FAB$^+$ *m*/*z* 258.0 $[M]^+$.

2-(4-{4-[4-(1,3-Dihydroxy-4,4,5,5-tetramethyl-imidazolidine-2-yl)phenyl]buta-1,3-diyn-1-yl}phenyl)-4,4,5,5-tetramethyl-imidazolidine-1,3-diol 3b. Following protocol A dibenzaldehyde **3a** (0.3 g, 1.19 mmol) was converted into imidazolidine **3b** after 3 h of refluxing with BHA in toluene in 97% yield (0.58 g). ^{1}H-NMR ($(CD_3)_2SO$, 250 MHz, 298 K, 128 scan), δ ppm: 1.28 (d, 24H, CH_3), 4.84 (s, 2H, –CH–), 7.92 (d, 4H, ^3J = 8 Hz), 8.11 (d, 4H, ^3J = 8 Hz). ^{13}C-NMR ($(CD_3)_2SO$, 63 MHz, 298K, 256 scan), δ ppm: 23, 69.7, 74.9, 82.3, 103.1, 123.6, 130.1, 134.0, 138.6.

2-(4-{4-[4-(1-Oxyl-3-oxo-4,4,5,5-tetramethyl-4H,5H-imidazolin-2-yl)-phenyl]buta-1,3-diyn-1-yl}phenyl)-4,4,5,5-tetramethyl-imidazoline-1-oxyl-3-oxo 3c. Biradical **3c** was obtained in 24% yield (0.140 g). M p 220–221 °C. UV-Vis ($CHCl_3$): λ/nm (ε/M^{-1} cm^{-1}) 607 (912), 349 (33844); (toluene) λ/nm (ε, $mol^{-1}\times$ cm^{-1}) 622 (578), 352 (71875). FT-IR (powder, ν/cm^{-1}) 3099, 3049 (w, ν_{C-H}, aromatic), 2991, 2940 (m, ν_{C-H}), 1602 (m, ν_{Ph}), 1543 (w), 1522 (m), 1481 (w), 1447 (m), 1428 (s), 1427(s), 1418 (*vs.*), 1386

(*vs.*, ν_{methyl}), 1365 (*vs.*, ν_{NO}), 1302 (*vs.*), 1212 (s), 1164 (s), 1141 (s), 1130 (*vs.*), 831 (*vs*, $\nu_{p\text{-sub-Ph}}$). (Calc. for $C_{30}H_{32}N_4O_4$: C, 70.29; H, 6.29; N, 10.93. Found: C, 70.30; H, 6.25; N, 10.90%).

4-[2-(4-Formylphenyl)ethynyl]benzaldehyde 4a (ref. 35). Starting compounds 4-ethynylbenzaldehyde **10** (0.2 g, 1.54 mmol), 4-bromobenzaldehyde **12** (0.284 g, 1.54 mmol) were transferred to a flame-dried flask in argon stream. Dry solvents mixture – DMF–NEt_3 (10 mL, 1 : 1) was added through the rubber septum. Solution was degassed using argon bubbles for 20 min, and then catalytic mixture of $Pd(PPh_3)_2Cl_2$ (54 mg, 0.077 mmol), PPh_3 (40 mg, 0.154 mmol), CuI (15 mg, 0.077 mmol) was added at once. The flask was sealed, moved into an oil bath and heated to 70 °C under argon for 12 h. The solvents were concentrated *in vacuo*. Purification using column chromatography (SiO_2, CH_2Cl_2) afforded the titled compound **4a** in 92% yield (0.33 g). ^{1}H-NMR ($CDCl_3$, 250 MHz, 298 K, 64 scan), δ ppm: 7.71, 7.90 (both dd 2H, $^3J = 8.2$ Hz, Ar-H), 10.04 (s, 2H, –CHO). ^{13}C-NMR (THF-d^8, 75 MHz, 298 K, 1725 scan), δ ppm: 92.4, 129.0, 130.1, 132.9, 137.5, 191.3. FAB$^+$ *m*/*z* 234.063 $[M]^+$.

2-(4-{2-[4-(1,3-Dihydroxy4,4,5,5-tetramethyl-imidazolidine-2-yl)phenyl]ethynyl}phenyl)-4,4,5,5-tetramethyl-imidazolidine-1,3-diol 4b. Following method A from 0.45 g (1.94 mmol) of dialdehyde **4a** bisimidazolidine **4b** was synthesized as 0.94 g (98%) of yellow powder. ^{1}H-NMR ($(CD_3)_2SO$, 250 MHz, 298 K, 105 scan), δ ppm: 1.05, 1.09 (both s 12 H, $-CH_3$), 4.54 (s, 2H, –CH–), 7.53 (w. s, 8H, Ar-H), 7.84 (w. s, 4H, –N–OH). ^{13}C-NMR ($(CD_3)_2SO$, 63 MHz, 298 K, 256 scan), δ ppm: 17.4, 24.5, 66.4, 88.2, 90.1, 121.6, 128.2, 131.0, 143.5. FAB$^+$ *m*/*z* 494.293 $[M]^+$.

2-(4-{2-[4-(1-Oxyl-3-oxo-4,4,5,5-tetramethyl-4H,5H-imidazolin-2-yl)phenyl]-ethynyl}phenyl)-4,4,5,5-tetramethyl-imidazoline-1-oxyl-3-oxo 4c. Oxidation of bisimidazolidine **4b** (0.94 g, 1.9 mmol) using procedure B gave 0.47 g (50%) of the dark-blue crystals of the biradical **4c**. UV-Vis (toluene): λ/nm (ε/M^{-1} cm^{-1}) 611 (868), 342 (59101). FT-IR (powder, ν/cm^{-1}) 3100 (w, ν_{C-H}, aromatic), 2989, 2943 (m, ν_{C-H}), 1677 (m), 1606 (s, ν_{Ph}), 1530 (w), 1484 (w), 1447 (m), 1422 (s), 1390(s, ν_{methyl}), 1365, 1356 (*vs.*, ν_{NO}), 1301 (*vs.*), 1211 (s), 1166 (s), 1131 (*vs.*), 833 (*vs.*, $\nu_{p\text{-sub-Ph}}$). (Calc. for $C_{28}H_{32}N_4O_4$: C, 68.83; H, 6.60; N, 11.47. Found: C, 68.67; H, 6.56; N, 11.37%).

Acknowledgements

The authors are pleased to acknowledge continued support from the Max Planck Society. This work was also supported by SFB TR49. We warmly thank Dr Giorgio Zopellaro for lively and helpful discussions.

Notes and references

1 Ch. Rüegg, K. Kiefer, B. Thielemann, D. F. McMorrow, V. Zapf, B. Normand, M. B. Zvonarev, P. Bouillot, C. Kollath, T. Giamarchi, S. Capponi, D. Poilblanc, D. Biner and K. W. Krämer, *Phys. Rev. Lett.*, 2008, **101**, 247202; V. Gurarie and J. T. Chalker, *Phys. Rev. Lett.*, 2002, **89**, 136801; T. Giamarchi, Ch. Rüegg and O. Tchernyshyov, *Nat. Phys.*, 2008, **4**, 198.

2 J. H. Osiecki and E. F. Ullman, *J. Am. Chem. Soc.*, 1968, **90**, 1078.

3 A. Caneschi, D. Gatteschi, P. Rey and R. Sessoli, *Inorg. Chem.*, 1988, **27**, 1756; A. Caneschi, D. Gatteschi, R. Sessoli and P. Rey, *Acc. Chem. Res.*, 1989, **22**, 392; C. Trein, L. Norel and M. Baumgarten, *Coord. Chem. Rev.*, 2009, **253**, 2342.

4 K. Inoue, T. Hayamizu, H. Iwamura, D. Hashizume and Y. Ohashi, *J. Am. Chem. Soc.*, 1996, **118**, 1803; S. Hiraoka, T. Okamoto, M. Kozaki, D. Shiomi, K. Sato, T. Takui and K. Okada, *J. Am. Chem. Soc.*, 2004, **126**, 58; C. Hirel, J. Pécaut, S. Choua, P. Turek, D. B. Amabilino, J. Veciana and P. Rey, *Eur. J. Org. Chem.*, 2005, 348.

5 T. Makarova and F. Palacio, *Carbon Based Magnetism*, Elsevier B. V., 2006; M. Tamura, Y. Nakazawa, D. Shiomi and M. Kinoshita, *Chem. Phys. Lett.*, 1991, **186**, 401.

6 *Stable Radicals: Fundamentals and Applied Aspects of Odd-Electron Compounds*, ed. R. G. Hicks, Wiley, Chichester, 2010.

7 S. Nishida, Y. Morita, K. Fukui, K. Sato, D. Shiomi, T. Takui and K. Nakasuji, *Angew. Chem.*, 2005, **117**, 7443; *Angew. Chem., Int. Ed.*, 2005, **44**, 7277; K. Sato, S. Nakazawa, R. Rahimi, T. Ise, S. Nishida, T. Yoshino, N. Mori and T. Takui, *J. Mater. Chem.*, 2009, **19**, 3739; Y. Morita, S. Suzuki, K. Sato and T. Takui, *Nat. Chem.*, 2011, **3**, 197.

8 H. Nishide and K. Oyaizu, *Science*, 2008, **319**, 737.

9 T. Sugawara, H. Komatsu and K. Suzuki, *Chem. Soc. Rev.*, 2011, **40**, 3105.

10 S. K. Pal, M. E. Itkis, F. S. Tham, R. W. Reed, R. T. Oakley and R. C. Haddon, *Science*, 2005, **309**, 281; A. Iwasaki, L. Hu, R. Suizu, K. Nomura, H. Yoshikawa, K. Awaga, Y. Noda, K. Kanai, Y. Ouchi, K. Seki and H. Ito, *Angew. Chem.*, 2009, **121**, 4082.

11 E. Coronado and A. J. Epstein, *J. Mater. Chem.*, 2009, **19**, 1670; E. Coronado and P. Day, *Chem. Rev.*, 2004, **104**, 5419.

12 G. Zoppellaro, A. Geies and M. Baumgarten, *Eur. J. Org. Chem.*, 2008, 1431; Y. Wang, L. Wang and L. Ma, *J. Mol. Struct.*, 2008, **877**, 138; H. Yamaguchi, S. Nagata, M. Tad, K. Iwase, T. Ono, S. Nishihara, Y. Hosokoshi, T. Shimokawa, H. Nojiri, A. Matsuo, K. Kindo and T. Kawakami, *Phys. Rev. B: Condens. Matter Mater. Phys.*, 2013, **87**, 125120.

13 E. Coronado, C. Gimenez-Saiz and C. J. Gomez-Garcıa, *J. Mater. Chem.*, 2008, **18**, 929; T. Yoshida and S. Kaizaki, *Inorg. Chem.*, 1999, **38**, 1054; K. Yamaguchi, M. Okumura, J. Maki, T. Noro, H. Namimoto, M. Nakano, T. Fueno and K. Nakasuji, *Chem. Phys. Lett.*, 1992, **190**, 353.

14 P. Siemsen and R. C. Livingston, *Angew. Chem., Int. Ed.*, 2000, **39**, 2632.

15 T. W. Greene, *Protective groups in organic synthesis*, 1991.

16 S. Takahashi, Y. Kuroyama, K. Sonogashira and N. Hagihara, *Chem. Commun.*, 1980, 627.

17 E. V. Tretyakov, S. Tolstikov and A. Mareev, *Eur. J. Org. Chem.*, 2009, **78**, 2548; E. V. Tretyakov and V. I. Ovcharenko, *Russ. Chem. Rev.*, 2009, **78**, 971.

18 G. R. Luckhurst and A. Hudson, *Mol. Phys.*, 1967, **13**, 409.

19 L. Catala, J. L. Moigne, N. Gruber and P. Turek, *Chem.–Eur. J.*, 2005, **11**, 2440; O. N. Chupakhin, I. A. Utepova, M. V. Varaksin and V. I. Ovcharenko, *J. Org. Chem.*, 2009,

74, 2870; S. V. Klyatskaya, E. V. Tretyakov and S. F. Vasilevsky, *Russ. Chem. Bull., Int. Ed.*, 2002, **51**, 128.
20 I. A. Grigor'ev, M. M. Mitasov, G. I. Shichikin and L. B. Volodarskii, *Seriya Khimicheskaya*, 1979, **11**, 2606; L. Rintoul, A. S. Micallef and S. E. Bottle, *Spectrochim. Acta, Part A*, 2008, **70**, 713.
21 E. Mostovich, PhD thesis, Novosibirsk, 2011.
22 T. Yoshida and S. Kaizaki, *Inorg. Chem.*, 1999, **38**, 1054.
23 A. Caneschi, D. Gatteschi and P. Rey, *Prog. Inorg. Chem.*, 1991, **39**, 331.
24 M. Shoji, K. Koizumi, Y. Kitagawa, T. Kawakami, S. Yamanaka, M. Okumura and K. Yamaguchi, *Chem. Phys. Lett.*, 2006, **432**, 343; T. Soda, Y. Kitagawa, T. Onishi, Y. Takano, Y. Shigeta, H. Nagao, Y. Yoshioka and K. Yamaguchi, *Chem. Phys. Lett.*, 2000, **319**, 223; K. Yamaguchi, F. Jensen, A. Dorigo and K. N. Houk, *Chem. Phys. Lett.*, 1988, **149**, 537.
25 O. Kahn, *Molecular Magnetism*, VCH, Weinheim-New York, 1993.
26 B. Bleaney and D. K. Bowers, *Proc. R. Soc. London, Ser. A*, 1952, **214**, 451.
27 F. M. Romero, R. Ziessel, M. Bonnet, Y. Pontillon, E. Ressouche, J. Schweizer, B. Delley, A. Grand and C. Paulsen, *J. Am. Chem. Soc.*, 2000, **122**, 1298.
28 C. Rancurel, N. Daro, O. Benedi Borobia, E. Herdtweck and J.-P. Sutter, *Eur. J. Org. Chem.*, 2003, **406**, 167.
29 K. Remović- Langer, E. Haussühl, L. Wiehl, B. Wolf, F. Sauli, N. Hasselmann, P. Kopietz and M. Lang, *J. Phys.: Condens. Matter*, 2009, **21**, 185013.
30 B. C. Watson, V. N. Kotov, M. W. Meise, D. W. Hall, G. E. Granroth, W. T. Montfrooij, S. E. Nagler, D. A. Jensen, R. Backov, M. A. Petruska, G. E. Fanucci and D. R. Talham, *Phys. Rev. Lett.*, 2001, **86**, 5168.
31 Ch. Wang, M. Kilitziraki, J. A. H. MacBride and I. D. W. Samuel, *Adv. Mater.*, 2000, **12**, 217.
32 G. Wulff, B. Heide and G. Helfmeier, *J. Am. Chem. Soc.*, 1986, **108**, 1089.
33 H. Lexy and T. Kauffmann, *Chem. Ber.*, 1980, **113**, 2749.
34 K. Maruyama and S. Kawabata, *Bull. Chem. Soc. Jpn.*, 1989, **62**, 3498.
35 A. Fürstner and Ch. Mathes, *Org. Lett.*, 2001, 221.